KEK Preprint 95-27
May 1995
H

A Measurement of Bose-Einstein Correlations in e^+e^- Annihilation at TRISTAN

AMY Collaboration

Submitted to Phys. Lett. B.

KEK Reports are available from:

Technical Information & Library
National Laboratory for High Energy Physics
1-1 Oho, Tsukuba-shi
Ibaraki-ken, 305
JAPAN

Phone: 0298-64-1171
Telex: 3652-534 (Domestic)
(0)3652-534 (International)
Fax: 0298-64-4604
Cable: KEK OHO
E-mail: LIBRARY@JPNKEKVX (Bitnet Address)
library@kekvax.kek.jp (Internet Address)

A Measurement of Bose-Einstein Correlations in e^+e^- Annihilation at TRISTAN

AMY Collaboration

S.K.Choi [a], R.C.Walker [b], A.Bodek [b], B.J.Kim [b], C.Velissaris [b], P.Kirk [c], A.Abashian [d], K.Gotow [d], M.E.Mattson [d], L.Piilonen[d], K.L.Sterner [d], C.Rosenfeld [e], L.Y.Zheng [e], C.A.Fry [f], R.Tanaka [f], R.E.Breedon [g], Winston Ko [g], R.L.Lander [g], J.Rowe [g], S.Kanda [h], S.L.Olsen [h], K.Ueno [h], K.Abe [i], Y.Fujii [i], Y.Kurihara [i], F.Liu [i], A.Maki [i], T.Nozaki [i], T.Omori [i], H.Sagawa [i], Y.Sakai[i], T.Sasaki [i], Y.Sugimoto [i], Y.Takaiwa [i], S.Terada [i], F.Kajino [j], T.Aso [k], K.Miyano [k], H.Miyata [k], N.Nakajima [k], K.Ohkubo [k], M.Oyoshi [k], M.Sato [k], M.Shirai [k], N.Takashimizu [k], Y.Yamashita [l], S.Schnetzer [m], J.Vinson [m], S.Behari [n], S.Kobayashi [n], A.Murakami [n], S.K.Sahu [n], J.S.Kang [o], D.Y.Kim [o], S.K.Kim [p], M.H.Lee [p], S.S.Myung [p], S.Ebara [q], and S.Matsumoto [q]

[a] *Gyeongsang National University, Chinju 660-701, South Korea*
[b] *University of Rochester, Rochester, NY 14627, USA*
[c] *Louisiana State University, Baton Rouge, LA 70803, USA*
[d] *Virginia Polytechnic Institute and State University, Blacksburg, VA 24061, USA*
[e] *University of South Carolina, Columbia, SC 29208, USA*
[f] *SSC Laboratory, Dallas, TX 75237, USA*
[g] *University of California, Davis, CA 95616, USA*
[h] *University of Hawaii, Honolulu, HI 96822, USA*
[i] *KEK, National Laboratory for High Energy Physics, Ibaraki 305, Japan*
[j] *Konan University, Kobe 658, Japan*
[k] *Niigata University, Niigata 950-21, Japan*
[l] *Nihon Dental College, Niigata 951, Japan*
[m] *Rutgers University, Piscataway, NJ 08854, USA*
[n] *Saga University, Saga 840, Japan*
[o] *Korea University, Seoul 136-701, South Korea*
[p] *Seoul National University, Seoul 151-742, South Korea*
[q] *Chuo University, Tokyo 112, Japan*

Abstract

Using e^+e^- annihilation events accumulated with the AMY detector at the TRISTAN collider, we have studied the Bose-Einstein correlations in the distributions of like-sign charged tracks. As reference samples we used the opposite-sign charged track pairs and mixed pairs, which are like-sign pairs synthesized from tracks belonging to different events. The results of the different reference samples give approximately 0.45 for the correlation strength and approximately 0.65 fm for the source size. Previous measurements of these parameters in e^+e^- annihilation at energies from CESR to LEP show remarkably flat dependence on $\sqrt{s}$. Our results conform well with this picture.

1 Introduction

Bose-Einstein correlations have been observed in multi-hadron events as an enhancement of the number of like-sign pion pairs in the region of low Q, where Q is the difference in four-momentum between members of the pair. The effect is a consequence of the constraint imposed by quantum field theory that the wave function of a system of identical bosons be symmetric under exchange. The experimental manifestations convey information about the size of the pion source and its chaoticity (the correlation strength), and these parameters, in turn, reflect on the mechanism of hadronization. Bose-Einstein correlations have been measured in many reactions, among them $\bar{p}p$, pp, πp, Kp, μp, νp, and e^+e^- [1]. Remarkably, the source size appears to be about 1.0 fm independent of the reaction. Furthermore, experiments on e^+e^- annihilation at energies from SPEAR to LEP suggest that the source size is also approximately independent of center-of-mass energy. Comparison of the correlation strength between reactions is problematic, but the energy dependence of this parameter in e^+e^- annihilation is illuminating. In a naive picture of hadronization in e^+e^-, quarks and gluons form a flux tube that ultimately disintigrates into hadrons. In this picture the pion source is far from being chaotic. One expects higher energy to result in a longer flux tube and therefore a reduction in the correlation strength. The observation is that the correlation strength, like the source size, is approximately energy independent. From the J/ψ energy to Υ threshold it drops from almost 1.0 to about 0.5, but thereafter it remains constant all the way to LEP energy.

The correlation function of two identical bosons is defined as

$$R(p_1, p_2) = \frac{\tilde{P}(p_1, p_2)}{P(p_1)P(p_2)}, \quad (1)$$

where $\tilde{P}$ is the joint probability density for observing one boson with momentum p_1 and the other with momentum p_2, and $P(p)$ is the single particle density. By a change of variables we recast R as a function of $Q \equiv |p_1 - p_2|$ and parametrize it as

$$R(Q) = 1 + \lambda e^{-Q^2 R_0^2}. \tag{2}$$

In this parametrization the source density has a gaussian profile $\exp(-r^2/2R_0^2)$ characterized by the rms radius R_0, and λ is the fraction of bosons that are chaotic and thus contributing to Bose-Einstein correlations. To extract R_0 and λ from data it is customary to compare the like-sign pion pairs with a reference sample for which the kinematic behavior is, ideally, the same and Bose-Einstein correlations are absent. The reference samples most commonly used are the opposite-sign pairs and the mixed pairs, in which the tracks of each like-sign pair are drawn from different events. The like-sign and opposite-sign samples share the correlations induced by global constraints like momentum and charge conservation and by the early stages of hadronization dynamics. The opposite-sign sample falls short of the ideal, however, because resonance production discriminates between like-sign and opposite-sign pairs and because the Coulomb force acts differently in the two cases. With respect to these two shortcomings the mixed pair sample offers considerable improvement. Having no resonance effects whatsoever makes it a good match to the like-sign sample for which resonance induced correlations are presumeably extremely weak. Having no Coulomb correlations whatsoever is more compatible than having Coulomb correlations with the wrong sign. A liability of the mixed pairs is that they do not preserve the correlations induced by global constraints. In principle we compensate for the differences between the like-sign pairs and a reference sample by normalizing each to a Monte Carlo simulation. The simulation does not incorporate Bose-Einstein correlations nor the Coulomb interaction but is supposed to account well for correlations induced by all other dynamical and instrumental effects. A "ratio of ratios," therefore, with adjustment for Coulomb effects, should reflect exclusively Bose-Einstein correlations.

2 The AMY Detector and Event Selection

The AMY detector incorporates three concentric cylindrical wire chambers for charged particle tracking within the bore of a 3 Tesla superconducting solenoid. The CDC, the outermost of the three tracking chambers has 25 layers of axial wires and 15 layers of stereo wires. Its acceptance in polar angle is the region $|\cos\theta| < 0.87$, and its resolution is $\Delta p_t/p_t \sim 0.7\% \times p_t(\mathrm{GeV/c})$ [2]. Also within the solenoid and surrounding the CDC

is a cylindrical electromagnetic calorimeter (SHC). It is an assembly of alternating layers of lead and proportional tubes having a total depth of 14.5 radiation lengths transverse to the beam direction. The SHC covers the angular range $|\cos\theta| < 0.75$, and its energy resolution is $\sigma_E/E = 23\%/\sqrt{E(\mathrm{GeV})} + 6\%$. [3] Surrounding the coil is an iron flux return yoke, which together with the coil and SHC constitutes a hadron filter of 9.8 nuclear absorption lengths. Outside the iron is the muon detection system (MUO) consisting of four planes of drift-tubes and a plane of scintillation counters. [4]

Two additional lead-proportional tube calorimeters, the ESC, cover the pole tips of the magnet. They detect Bhabha events over the angular interval from $\theta = 12°$ to $25°$, from which we determine the luminosity. The data on which we base this analysis corresponds to an integrated luminosity of 202 pb^{-1}.

The selection criteria that define the sample of multihadron events are the following.

1. The CDC must record at least six charged tracks within $|\cos\theta| \leq 0.85$ that have a minimum of of nine hits on axial wires and a minimum of eight hits on stereo wires. The fit of a helix to the data of each track must yield $\chi^2_{r\phi} \leq 8.0$ and $\chi^2_z \leq 6.0$. The fitted trajectories must have $|D_0|$ less than 5 cm and $|Z_0|$ less than 9 cm where $|D_0|$ is the distance from the beam axis of the point of closest approach and $|Z_0|$ is the axial coordinate of this point. Finally the qualifying tracks must not be curling (see below) and must fail the criteria for electron and muon tracks. The electron criteria require that a track a) have momentum p greater than 2.5 GeV, b) project to a position in the SHC that is within 2° in both θ and ϕ of a "cluster" of energy deposition, and c) have $0.6 < E_c/p < 1.5$ where E_c is the energy of the associated cluster. The muon criteria require that the projection of a CDC track to the MUO be no more that 1.0 m from a MUO track reconstructed from hits in at least three of the four planes of drift tubes.

2. The energy deposited in the SHC must exceed 5.0 GeV. When summing the energies of clusters to obtain the energy deposited, we include a cluster with energy E_c only if $|\cos\theta| \leq 0.73$ and $E_c > 0.2$ GeV. We exclude a cluster if $E_c > 0.5$ GeV and more than 95% of the cluster energy comes from a single layer or if $E_c > 1.0$ GeV and the cluster is near the projection of a charged track.

3. The sum of the energies of measured charged and neutral particles, E_{vis}, must exceed the beam energy.

4. $|P_{\mathrm{bal}}|/E_{\mathrm{vis}} < 0.4$ where P_{bal} is the axial component of the net momentum of the well measured charged and neutral particles.

These criteria eliminated background events from beam-wall, beam-gas, $\tau^+\tau^-$, two-photon, and radiative Bhabha events and also suppressed events in which substantial energy was emitted along the beam axis where it was invisible to the detector. Less than 0.4% of pairs include a poorly measured track, and the fraction is independent of Q. At this level we considered such pairs inconsequential and ignored them. The number of events that satisfied these selection criteria was 17,578.

The track reconstruction software produces certain artifacts that are inimical to this analysis. Particles emitted at polar angles near 90° with transverse momentum p_t less than 350 MeV/c curl up within the CDC. The track finding algorithm sometimes interprets successive segments of such trajectories as independent tracks. Most commonly the algorithm produces two tracks having opposite sign, opening angle close to 180°, and nearly identical momenta. At a much lower rate the outcome is a like-sign pair with opening angle near 0°. To suppress these artifacts we excluded opposite-sign pairs from further analysis when both tracks had $p_t < 400$ MeV/c, difference in p_t less than 40 MeV/c, and opening angle greater than 170°. Similarly, we excluded like-sign pairs when the tracks had $p_t < 400$ MeV/c, difference in p_t less than 40 MeV/c, and opening angle less than 10°. Occasionally the reconstruction algorithm assembles two tracks from the hits generated by a single particle that does not curl. The ersatz pair necessarily has very small Q and would be a damaging contaminant in the like-sign sample. We suppress these by excluding pairs when the difference in p_t is less than 40 MeV/c and the opening angle is less than 3°.

When both members of a track pair have high momentum, energy conservation has a greater influence on the Q distribution. In principle the ratio-of-ratios approach will suppress sensitivity to this effect, but we improve the ruggedness of our results if we nonetheless cast out high momentum tracks. In forming track pairs we rejected tracks with momentum above 3.0 GeV. We believe this limit to be lower than necessary to eliminate phase space induced correlations. Since only a small proportion of tracks exceed 3.0 GeV, the cost in statistical significance is negligible.

A Monte Carlo sample of hadronic events was generated using LUND JETSET 7.3 with parton shower and string fragmentation algorithms. A simulation program rendered the response of the AMY detector to these events. We applied to this sample the same selection criteria that we applied to the data, and 28,571 events survived.

3 Calculation of Correlation Functions

For each multihadron event we formed all possible pairs of tracks and calculated the Q of each. Figure 1(a) and 1(b) show the distributions of Q for like-sign pairs and opposite-sign pairs in the data. Figure 1(d) and 1(e) show the corresponding distributions for the simulated sample. A typical hadronic event presents more pairs of opposite sign than like sign (e.g. 100 opposite-sign and 90 like-sign pairs in an event with 10 tracks of each charge). Overall we observe 15% more opposite-sign pairs, and this excess is Q-dependent.

Mesons that decay close to the interaction point, e.g. ρ^0 and K_s, enhance the population of opposite-sign pairs in the range of Q from 0.4 to 0.8 GeV/c. (The Q of a pair of pions is related to the mass of the pair according to

$$Q_{ij} = \sqrt{M_{ij}^2 - 4m_\pi^2}\,.) \tag{3}$$

The effect is evident in Figure 1. The enhancement is larger in the Monte Carlo sample than in the data. We have not understood this discrepancy, and we will make an accommodation for it when we estimate systematic errors.

Our method for constructing the mixed pairs is based on the method developed by Mark II [5]. We used the jet clustering algorithm developed by the JADE collaboration [6]. For the y_{cut} parameter of the clustering algorithm we used 0.03. After assigning tracks to clusters in all of the events we selected pairs of kinematically similar clusters. We considered two clusters, A and B, to be similar when (a) they originated in events having the same number of clusters, (b) the two clusters have the same number of charged tracks, (c) $|(W_A - W_B)/(W_A + W_B)| < 0.25$ where

$$W_\Gamma = \sum_{i \in \text{Cluster } \Gamma} |\mathbf{p}_i| \tag{4}$$

and the sum runs over the neutral as well as the charged members of the cluster, and (d) $|\theta_A - \theta_B| \leq 5°$ where θ is the polar angle of the cluster axis (direction of the cluster momentum). For one cluster of each matched pair we reoriented the tracks as a group so that the cluster axes were parallel. We then formed all pairs of tracks with like sign taking one track from cluster A, the other from cluster B. The Q distributions of the mixed pairs appear in Figure 1(c) for the AMY data and in Figure 1(f) for the Monte Carlo sample. The good agreement between data and simulation is evidence that the Monte Carlo reproduces at least the gross features dictated by multiplicity, jet structure, and acceptance.

From the Q distributions we calculated the correlation function as follows,

$$R_{+-}(Q) = \frac{[N_{\pm\pm}(Q)/N_{+-}(Q)]_{\rm data}}{[N_{\pm\pm}(Q)/N_{+-}(Q)]_{\rm MC}} \qquad (5)$$

$$R_{\rm mix}(Q) = \frac{[N_{\pm\pm}(Q)/N_{\rm mix}(Q)]_{\rm data}}{[N_{\pm\pm}(Q)/N_{\rm mix}(Q)]_{\rm MC}}, \qquad (6)$$

where the subscripts $\pm\pm$, $+-$, and "mix" denote like-sign, opposite-sign, and mixed pairs respectively. The numerators were computed from the data and the denominators from the simulated sample. The $R_{+-}(Q)$ and $R_{\rm mix}(Q)$ appear in Figure 2. In principle these distributions depart from uniformity only as a result of phenomena not modeled in the simulation. The significant effects absent from the Monte Carlo are the Bose-Einstein correlations and the Coulomb interaction, and the manifestations of the latter are comparatively weak. Therefore the Bose-Einstein correlations must account for the rise in R at $Q < 0.3$ GeV.

4 Results and discussion

We parametrized the distributions $R_{+-}(Q)$ and $R_{\rm mix}(Q)$ using the forms

$$R_{+-}(Q) = N_0(1 + f_\pi(Q)\lambda e^{-R_0^2Q^2})(1+\gamma Q)G_{\pm\pm}(Q)/G_{+-}(Q) \qquad (7)$$

$$R_{\rm mix}(Q) = N_0(1 + f_\pi(Q)\lambda e^{-R_0^2Q^2})(1+\gamma Q)G_{\pm\pm}(Q) \qquad (8)$$

R_0 and λ are the parameters of the Bose-Einstein correlations. The term involving γ accounts for the slow rise in R at large Q, which reflects the global conservation of charge and energy. The normalization constant N_0 allows for the unequal number of like-sign and opposite-sign pairs and for the corresponding differential between like-sign and mixed pairs. The AMY detector does not distinguish charged pions from charged kaons and protons. The function $f_\pi(Q)$ accommodates the heterogeneous pairs, to which Bose-Einstein correlations do not apply. From the Monte Carlo sample we determined the fraction of like-sign pairs that are indeed pion pairs,

$$f_\pi(Q) = N_{\pi\pi}(Q)/N_{\pm\pm}(Q). \qquad (9)$$

We parametrized this function as

$$f_\pi(Q) = 0.719 - 0.070\,Q + 0.056\,Q^2 - 0.020\,Q^3. \qquad (10)$$

which gives $f_\pi(Q)$ values of about 68% with only a mild dependence on Q. The Gamow factors $G_{\pm\pm}$ and G_{+-} [7] describe the perturbation in $N_{\pm\pm}$ and N_{+-} induced by the

Coulomb force. $G_{\pm\pm}(Q) = 2\pi\xi/(\exp(2\pi\xi) - 1)$, and $G_{+-}(Q) = 2\pi\xi/(1 - \exp(-2\pi\xi))$ where $\xi = \alpha m_\pi/Q$, $\alpha = 1/137$ is the fine structure constant, and m_π is the pion mass. At $Q = 0.1$ GeV, $G_{\pm\pm}$ and G_{+-} are 0.97 and 1.03, respectively. Photon conversions ($\gamma \to e^+e^-$) and curling tracks, to the extent that they escape our selection cuts, would accumulate at very small Q. We are not confident that the simulation accurately models this leakage, and to improve immunity to such contamination our standard fit excludes the region $Q < 60$ MeV/c. The parameters obtained for the standard fit appear in row (a) of Table 1.

We calculated two additional fits for the purpose of assessing systematic errors. First, to estimate the impact of the inaccurate simulation of the resonance region we excluded the interval $0.4 < Q < 0.8$ GeV in the fit for $R_{+-}(Q)$. (Resonances do not effect $R_{\rm mix}$.) The parameters of this fit are given in row (b) of Table 1. To accommodate the difference between this fit and the standard fit we alloted 4.7% to the systematic error of λ. Next we investigated the effect of the ambiguity in the Coulomb induced correlations. As pointed out by Bowler [8], the Gamow factors might overstate the effect of the Coulomb force because a pion originating in the primary interaction is likely to be spatially well separated from a second pion originating in the decay of a long-lived secondary (e.g. η, η', ω, K_0^*, D, and B). According to the simulation, pairs having this character contribute 70% of all the pairs for $0.06 < Q < 0.2$ GeV/c. Therefore, in a second variation on the standard fit, we replaced the Gamow factors G by G' where $|1 - G'| = 0.3|1 - G|$. Row (c) of Table 1 gives the results for this exercise. To accommodate the shift in parameters from the standard fit we allotted to the systematic error in λ based on the opposite-sign pairs 10%, and to the λ based on the mixed pairs 7.0%. To the systematic error in R_0 we allotted 2.6% for both of the reference samples. We asigned 1% systematic error to both λ and R_0 due to the effect of the momentum resolution. This was determined from a study of smearing of the correlations due to the momentum resolution using the Bose-Einstein parameters determined from the standard fit.

For the overall systematic error we took the sum in quadrature of the errors estimated for resonance region inaccuracy, Coulomb interaction uncertainty, and momentum resolution. We elected not to estimate the systematic error from the difference in results obtained using the two reference samples. Some part of this difference may result from the different dynamics of the reference samples as discussed earlier. Some readers will have an interest in the separately stated results of the two methods and should have the benefit of separately stated systematic errors.

Table 1: Results of fits. Row (a), standard fit as described in the text, (b) fit with the resonance region $0.4 < Q < to0.8$ GeV/c excluded, and (c) fit with Coulomb adjustment weighted by 30%.

	λ		R_0		χ^2/dof	
	R_{+-}	R_{mix}	R_{+-}	R_{mix}	R_{+-}	R_{mix}
(a)	0.470±0.047	0.392±0.041	0.730±0.050	0.582±0.062	78.7/93.	90.2/93.
(b)	0.448±0.047		0.731±0.049		76.9/73.	
(c)	0.422±0.045	0.365±0.040	0.719±0.052	0.567±0.063	80.1/93.	89.7/93.

Our final results for λ and R_0 at $\sqrt{s}$=58.0 GeV are

$$\lambda = 0.470 \pm 0.047 \pm 0.053, \qquad R_0 = 0.730 \pm 0.050 \pm 0.020 \text{ fm} \tag{11}$$

when we use the opposite-sign pairs as the reference sample, and

$$\lambda = 0.392 \pm 0.041 \pm 0.027, \qquad R_0 = 0.582 \pm 0.062 \pm 0.016 \text{ fm} \tag{12}$$

when we use the mixed pairs as the reference sample. The first error quoted for each parameter is statistical, and the second is systematic. The results obtained using the two reference samples are not significantly different.

In Figure 3 we plot our results for λ together with published measurements at other energies [5, 9, 10, 11, 12, 13, 14]. The measurements were assigned to part (a) or to part (b) of the figure according to the type of reference sample used. Figure 4 shows the corresponding plots for R_0. The results reported here conform well with the $\sqrt{s}$-dependence suggested by previous measurements. The source size R_0, at approximately 0.8 fm, is nearly energy independent from charm threshold to the Z. The λ parameter is sensitive to the fraction of pions originating in the primary source region as opposed to those produced in the decays of long-lived resonances and heavy mesons. The constancy of λ from 10 to 90 GeV is thus consistent with approximate energy independence of $\eta(s)$, the fraction of like-sign pion pairs that originate in the prompt source. According to our simulations $\eta(s)$ hovers around 30% at TRISTAN energies and below, and it is 24% at LEP energy [14]. The value of λ, on the other hand, presents a conundrum. Our expectation is that $\lambda \leq \eta(s)$ with equality holding for a maximally chaotic prompt source. The observations, however, place λ at about 0.5, significantly exceeding $\eta(s)$ as determined from the simulation.

References

[1] B. Lorstad, Int. Jour. Mod. Phys.**A4**, 2861 (1989).

[2] K. Ueno, *et al.*, Nucl. Instr. and Meth. **A323**, 601 (1992).

[3] A. Abashian, *et al.*, Nucl. Instr. Meth. **A317**, 75 (1992).

[4] F. Liu, *et al.*, Phys. Rev. **D49**, 4339 (1994).

[5] I. Juricic, *et al.* (Mark II Collab.), Phys. Rev. D **39**, 1 (1989).

[6] W. Bartel, *et al.* (JADE Collab.), Z. Phys. **C33**, 23 (1986).

[7] M. Gyulassy, *et al.*, Phys. Rev. **C20**, 2267 (1979).

[8] M. G. Bowler, OUNP-91-23 (1991).

[9] P. Avery, *et al.* (CLEO Collab.), Phys. Rev. **D32**, 2294 (1985). Their analysis used the tranverse component of Q^2 instead of Q^2. They mention, however, that the longitudinal component contributes very little. Therefore we include their results in our plots without modification.

[10] H. Aihara, *et al.* (TPC Collab.), Phys. Rev. **D31**, 996 (1985).

[11] M. Althoff, *et al.* (TASSO Collab.), Z. Phys. **C30**, 355 (1986). These authors did not compensate for heterogeneous pairs (e.g. a π and a K) nor did they adjust for the Coulomb interaction. They did make a correction for long-lived particles. In the preparation of Figure 3(a) we reversed this correction and used $\lambda = 0.35 \pm 0.05$.

[12] P.D. Acton, *et al.* (OPAL Collab.), Phys. Lett. **B267**, 143 (1991). This analysis includes only the Coulomb correction. The systematic error, however, includes a contribution for hererogeneous pairs.

[13] P. Abreu, *et al.* (DELPHI Collab.), Phys. Lett. **B286**, 201 (1992).

[14] D. Decamp, *et al.* (ALEPH Collab.), Z. Phys. **C54**, 75 (1992).

Figure Captions.

Figure 1 The Q distribution of like-sign pairs, opposite-sign pairs, and mixed pairs for both data (a through c), and for the Monte Carlo sample (d through f).

Figure 2 The correlation functions $R_{+-}(Q)$ and $R_{mix}(Q)$. The curves are our standard fits, and their parameters are shown at upper right.

Figure 3 The λ parameter obtained in this experiment and several others *vs.* center-of-mass energy. In (a) the reference sample is opposite-sign pairs, and in (b) the reference sample is mixed pairs. Arrows standing on the horizontal axis indicate the thresholds for charm and bottom production and the Z resonance.

Figure 4 The R_0 parameter obtained in this experiment and several others *vs.* center-of-mass energy. In (a) the reference sample is opposite-sign pairs, and in (b) the reference sample is mixed pairs.

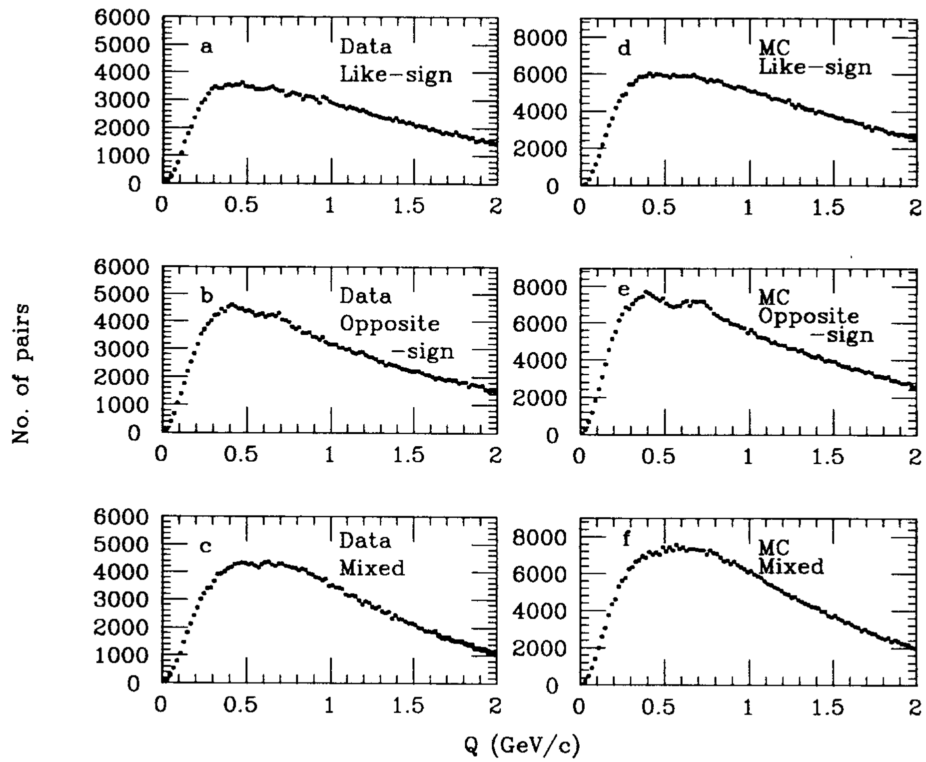

Figure 1

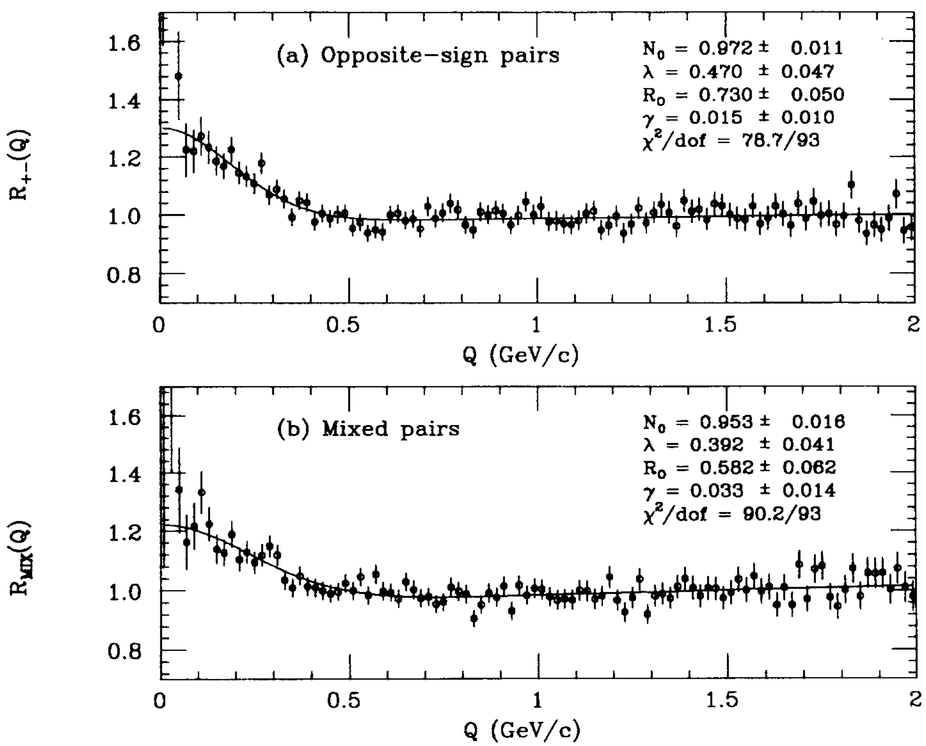

Figure 2

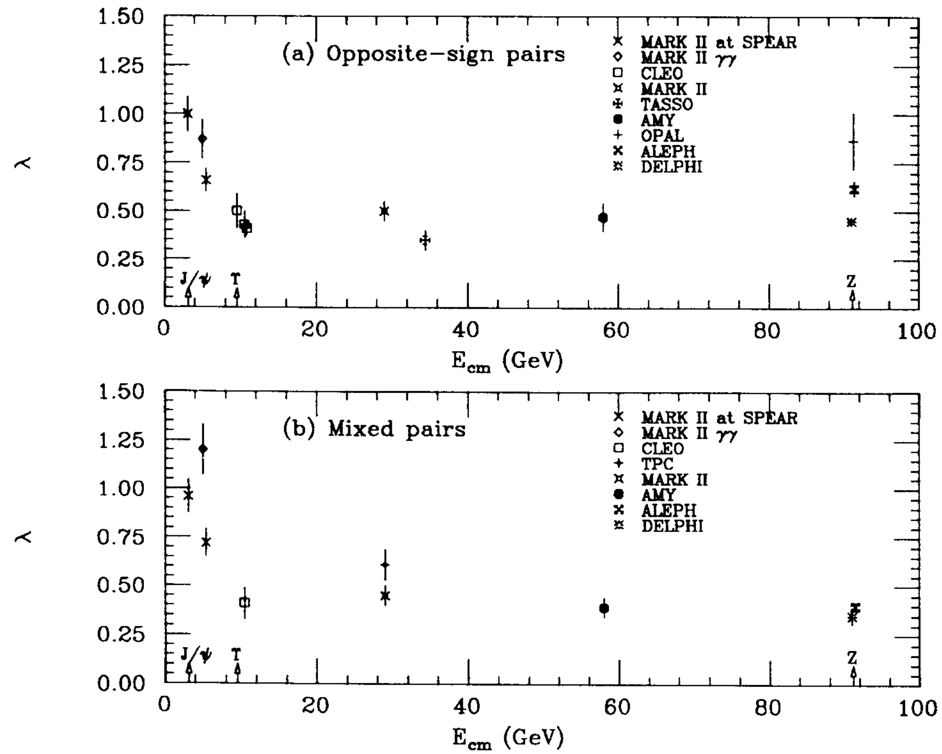

Figure 3

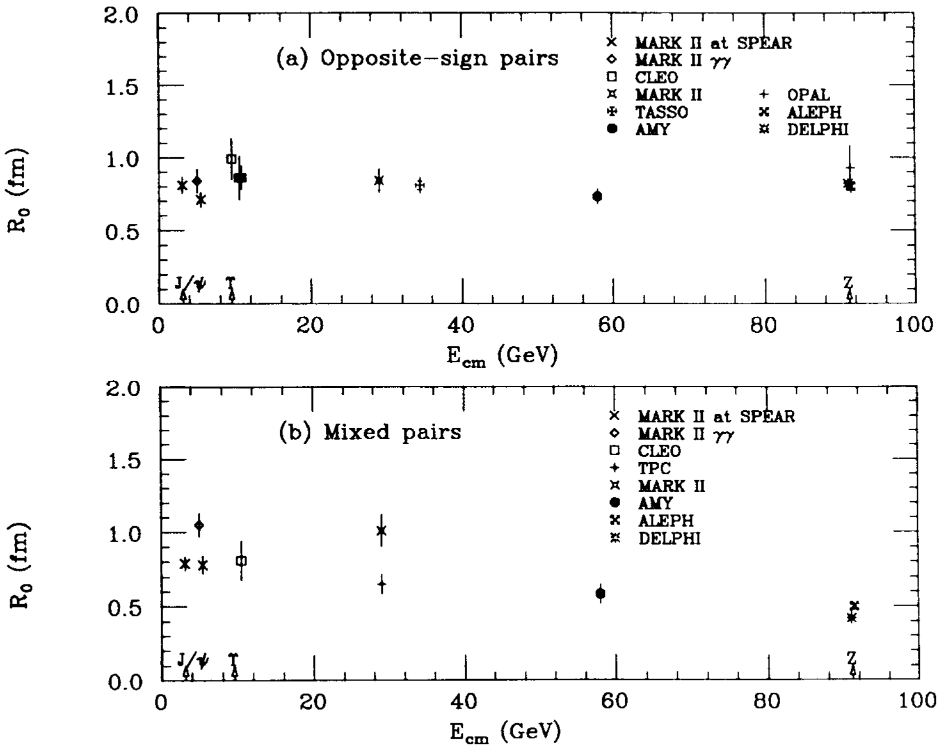

(a) Opposite-sign pairs
MARK II at SPEAR
MARK II γγ
CLEO
MARK II
TASSO
AMY
OPAL
ALEPH
DELPHI
R₀ (fm)
E_cm (GeV)
J/ψ
Υ
Z
(b) Mixed pairs
MARK II at SPEAR
MARK II γγ
CLEO
TPC
MARK II
AMY
ALEPH
DELPHI

Figure 4